ASIAN JOURNAL OF CIVIL ENGINEERING (BUILDING AND HOUSING) VOL. 12, NO. 4 (2011)
PAGES 487-509

# SHAPE AND SIZE OPTIMIZATION OF TRUSS STRUCTURES WITH FREQUENCY CONSTRAINTS USING ENHANCED CHARGED SYSTEM SEARCH ALGORITHM

A. Kaveh* and A. Zolghadr
Centre of Excellence for Fundamental Studies in Structural Engineering, Iran University of Science and Technology, Narmak, Tehran-16, Iran

**Received:** 6 September 2010, **Accepted:** 28 December 2010

## ABSTRACT

Natural frequencies are relatively easy parameters to obtain and they represent useful information about the dynamic behavior of structures. Controlling these parameters can help the designer to minimize destructive effect of dynamic loading on the structure.

Apart from the aforementioned practical application, weight optimization of the structures with frequency constraints is a notorious problem because of its highly non-linear behavior. Thus form a challenging field to apply the optimization techniques.

In this paper, the charged system search algorithm and its enhanced version are utilized to optimize various truss structures with multiple frequency constraints. The examples investigated here, are well-known benchmark problems. The results show that the presented algorithms perform better than other optimization techniques for most of the benchmark examples.

**Keywords:** Enhanced charged system search; shape and size optimization; truss structures; frequency constraint

## 1. INTRODUCTION

It is well known that the natural frequencies are fundamental parameters affecting the dynamic behavior of the structures. Therefore, some limitations should be imposed on the natural frequency range to reduce the domain of vibration and also to prevent the resonance phenomenon in dynamic response of structures [1]. On the other hand, engineering structures are often supposed to be as light as possible. Thus a frequency constraint weight optimization process should be performed to obtain these two aims simultaneously.

Frequency constraints are highly non-linear, non-convex and implicit with respect to the

*E-mail address of the corresponding author: alikaveh@iust.ac.ir (A. Kaveh)

design variables [2]. Therefore mathematical programming approaches would be hard to apply and time-consuming in these optimization problems. Furthermore, a good starting point is vital for these methods to be executed successfully [3] and they may converge to the local optima. Simultaneous consideration of sizing and shape variables together with the vibration mode switching phenomenon which usually occurs while minimizing the weight may cause some convergence difficulties. Hence, utilizing a global search optimization technique which obviates these difficulties seems to be inevitable.

As a newly developed type of meta-heuristic algorithm, the charged system search (CSS) is introduced by Kaveh and Talatahari for design of structural problems [3]. This method utilizes the governing laws of Coulomb and Gauss from electrostatics and the Newtonian laws of mechanics. Inspired by these laws, a model is created to formulate the structural optimization method. The CSS algorithm contains a number of agents which are called charged particles (CPs). Each CP is considered as a charged sphere which exerts an electric force on other CPs according to the Coulomb and Gauss laws. The resultant forces and the laws of motion determine the new location of the CPs [4]. Charged system search is proved to be competent in structural optimization problems considering stresses and displacements as the constraints. This algorithm and its enhanced form proposed by Kaveh and Talatahari [5] will be used here to optimize truss structures for shape and size with frequency constraints.

The remainder of this paper is organized as follows: In section 2, truss optimization problem with frequency constraints is stated. A brief introduction to CSS and its enhanced form is presented in section 3. Some numerical examples are studied in section 4. Finally some concluding remarks are provided in section 5.

## 2. PROBLEM STATEMENT

In a truss optimization problem with frequency constraints, the goal is to minimize the weight of the structure while satisfying multiple constraints on natural frequencies. Cross-sectional areas of the members along with the coordinates of some nodes are considered to be the design variables and assumed to change continuously. The connectivity information of the structure is predefined and kept unchanged during the optimization process. A lower and upper bound may also be prescribed for each variable. The optimization problem can be stated mathematically as follows:

$$\begin{array}{c} \text{Find } X=[x_1,x_2,x_3,..,x_n] \\ \text{to minimizes Mer } (X) = f(X) \times f_{penalty}(X) \\ \text{subjected to} \\ \omega_j \le \omega_j^* \quad \text{for some natural frequencies j} \\ \omega_k \ge \omega_k^* \quad \text{for some natural frequencies k} \\ x_{imin} \le x_i \le x_{imax} \end{array} \tag{1}$$

where X is the vector containing the design variables, including both nodal coordinates and cross-sectional areas. Here n is the number of variables which is usually chosen with respect to the symmetry and practice requirements. Mer(X) is the merit function; f(X) is the cost function, which is taken as the weight of the structure; $f_{penalty}(X)$ is the penalty function which results from the violations of the constraints corresponding to the response of the structure [8]; $\omega_j$ is the ith natural frequency of the structure and $\omega_j^*$ is its upper bound. $\omega_k$ is the kth natural frequency of the structure and $\omega_k^*$ is its lower bound. $x_{imin}$ and $x_{imax}$ are the lower and upper bounds of the design variable $x_i$, respectively.

The cost function is expressed as

$$f(X) = \sum_{i=1}^{nm} \rho_i L_i A_i \tag{2}$$

where $\rho_i$ is the material density of member i; $L_i$ is the length of member i; and $A_i$ is the cross-sectional area of member i.

The penalty function is defined as [3]:

$$f_{penalty}(X) = (1+\varepsilon_1 . v)^{\varepsilon_2}, \; v = \sum_{i=1}^{q} v_i \tag{3}$$

where q is the number of frequency constraints. If the ith constraint is satisfied $v_i$ will be taken as zero, if not it will be taken as

$$v_i = |\, 1 - \left( \frac{\omega_i}{\omega^*_i} \right) | \tag{4}$$

The parameters $\varepsilon_1$ and $\varepsilon_2$ are selected considering the exploration and the exploitation rate of the search space.

## 3. THE CHARGED SYSTEM SEARCH

*3.1 The standard CSS*

Recently an efficient optimization algorithm, known as the charged system search, has been proposed by Kaveh and Talatahari [3]. This algorithm is based on electrostatics and Newtonian mechanics laws.

The Coulomb and Gauss laws provide the magnitude of the electric field at a point inside and outside a charged insulating solid sphere, respectively, as follows [6]:

$$E_{ij} = \begin{cases} \dfrac{k_e q_i}{a^3} r_{ij} & \text{if } r_{ij} < a \\ \dfrac{k_e q_i}{r_{ij}^2} & \text{if } r_{ij} \ge a \end{cases} \tag{5}$$

where $k_e$ is a constant known as the Coulomb constant; $r_{ij}$ is the separation of the centre of sphere and the selected point; $q_i$ is the magnitude of the charge; and "a" is the radius of the charged sphere. Using the principle of superposition, the resulting electric force due to N charged spheres is equal to [3]:

$$F_j = k_{eq} \sum_{i=1}^{N} \left( \frac{q_i}{a^3} r_{ij} . i_1 + \frac{q_i}{r_{ij}^2} . i_2 \right) \frac{r_i - r_j}{\| r_i - r_j \|} \quad \begin{cases} i_1 = 1, i_2 = 0 \Leftrightarrow r_{ij} < a \\ i_1 = 0, i_2 = 1 \Leftrightarrow r_{ij} \geq a \end{cases} \tag{6}$$

Also, according to Newtonian mechanics, we have [6]:

$$\Delta r = r_{new} - r_{old} \tag{7}$$

$$v = \frac{r_{new} - r_{old}}{\Delta t} \tag{8}$$

$$a = \frac{v_{new} - v_{old}}{\Delta t} \tag{9}$$

where $r_{old}$ and $r_{new}$ are the initial and final positions of the particle, respectively; v is the velocity of the particle; and a is the acceleration of the particle . Combining the above equations and using Newton's second law, the displacement of any object as a function of time is obtained as [6]:

$$r_{new} = \frac{1}{2} \frac{F}{M} . \Delta t^2 + v_{old} + r_{old} \tag{10}$$

Inspired by the above electrostatic and Newtonian mechanics laws, the pseudo-code of the CSS algorithm is presented as follows [7]:

*Level 1: Initialization*

Step 1. Initialization. Initialize the parameters of the CSS algorithm. Initialize an array of charged particles (CPs) with random positions. The initial velocities of the CPs are taken as zero. Each CP has a charge of magnitude (q) defined considering the quality of its solution as:

$$q_i = \frac{fit(i) - fit_{worst}}{fit_{best} - fit_{worst}} \qquad i = 1,2,\ldots N \tag{11}$$

where $fit_{best}$ and $fit_{worst}$ are the best and the worst fitness of all the particles; fit(i) represents the fitness of agent i. The separation distance $r_{ij}$ between two charged particles is defined as:

$$r_{ij} = \frac{\left\| X_i - X_j \right\|}{\left\| \frac{(X_i + X_j)}{2} - X_{best} \right\| + \varepsilon} \tag{12}$$

where $X_i$ and $X_j$ are the positions of the ith and jth CPs, respectively; $X_{best}$ is the position of the best current CP; and ε is a small positive to avoid singularities.

Step 2. CP ranking. Evaluate the values of the fitness function for the CPs, compare with each other and sort them in increasing order.

Step 3. CM creation. Store the number of the first CPs equal to charged memory size (CMS) and their related values of the fitness functions in the charged memory (CM).

*Level 2: Search*

Step 1. Attracting force determination. Determine the probability of moving each CP toward the others considering the following probability function:

$$P_{ij} = \begin{cases} 1 & \frac{fit(i) - fit_{best}}{fit(j) - fit(i)} > rand \vee fit(j) > fit(i) \\ 0 & else \end{cases} \tag{13}$$

and calculate the attracting force vector for each CP as follows:

$$F_{ij} = q_j \sum_{i,i \neq j} \left( \frac{q_i}{a^3} r_{ij} \,.\, i_1 + \frac{q_i}{r_{ij}^2} \,.\, i_2 \right) p_{ij} \left( X_i - X_j \right) \quad \begin{cases} j = 1,2,\ldots,N \\ i_1 = 1, i_2 = 0 \Leftrightarrow r_{ij} < a \\ i_1 = 0, i_2 = 1 \Leftrightarrow r_{ij} \geq a \end{cases} \tag{14}$$

where $F_j$ is the resultant force affecting the jth CP.

Step 2. Solution construction. Move each CP to the new position and find its velocity using the following equations:

$$X_{j,new} = rand_{j1} \,.\, k_a \,.\, \frac{F_j}{m_j} \,.\, \Delta t^2 + rand_{j2} \,.\, k_v \,.\, V_{j,old} \,.\, \Delta t + X_{j,old} \tag{15}$$

$$V_{j,new} = \frac{X_{j,new} - X_{j,old}}{\Delta t} \tag{16}$$

where $rand_{j1}$ and $rand_{j2}$ are two random numbers uniformly distributed in the range (1,0); $m_j$ is the mass of the CPs, which is equal to $q_j$ in this paper. The mass concept may be useful for developing a multi-objective CSS. Δt is the time step, and it is set to 1. $k_a$ is the acceleration coefficient; $k_v$ is the velocity coefficient to control the influence of the previous velocity. In this paper $k_v$ and $k_a$ are taken as:

$$k_a=c_1(1+iter/iter_{max}), \quad k_v= c_2(1-iter/iter_{max}) \tag{17}$$

where $c_1$ and $c_2$ are two constants to control the exploitation and exploration of the algorithm; iter is the iteration number and $iter_{max}$ is the maximum number of iterations.

Step 3. CP position correction. If each CP exits from the allowable search space, correct its position using the HS-based handling as described by Kaveh and Talatahari [3,8].

Step 4. CP ranking. Evaluate and compare the values of the fitness function for the new CPs; and sort them in an increasing order.

Step 5. CM updating. If some new CP vectors are better than the worst ones in the CM, in terms of their objective function values, include the better vectors in the CM and exclude the worst ones from the CM.

*Level 3: Controlling the terminating criterion*

Repeat the search level steps until a terminating criterion is satisfied.

### *3.2 An enhanced CSS*

In addition to the standard CSS, an enhanced CSS which is recently proposed by Kaveh and Talatahari [5] is used. In the standard CSS algorithm, when the calculations of the amount of forces are completed for all CPs, the new locations of agents are determined. Also CM updating is fulfilled after moving all CPs to their new locations. All these conform to discrete time concept. In the optimization problems, this is known as iteration. On the contrary, in the enhanced CSS, time changes continuously and after creating just one solution, all updating processes are performed. Using this enhanced CSS, the new position of each agent can affect the moving process of the subsequent CPs while in the standard CSS unless an iteration is completed, the new positions are not utilized. All other aspects of the enhanced CSS are similar to the original one.

## 4. NUMERICAL EXAMPLES

### *4.1 A ten-bar truss*

A ten-bar planar truss, as depicted in Figure 1, is a well-known benchmark problem in the field of weight optimization of the structures with frequency constraints. This is merely a size optimization problem and the predefined shape of the structure is kept unchanged during the optimization process. The cross-sectional area of each of the members is considered to be an independent variable. A non-structural mass of 454.0 kg is attached to the free nodes. Table 1 shows the material properties, variable bounds, and frequency constraints for this example. This problem has been investigated by Grandhi and Venkayya [9] using the optimality algorithm. Sedaghati, et al. [10] have solved it by sequential quadratic programming and the finite element force method. Wang et al. [11] have used an evolutionary node shift method, and Lingyun et al. [12] have used a niche hybrid genetic algorithm to optimize this structure. Gomes [13] has analyzed this problem using the particle swarm algorithm.

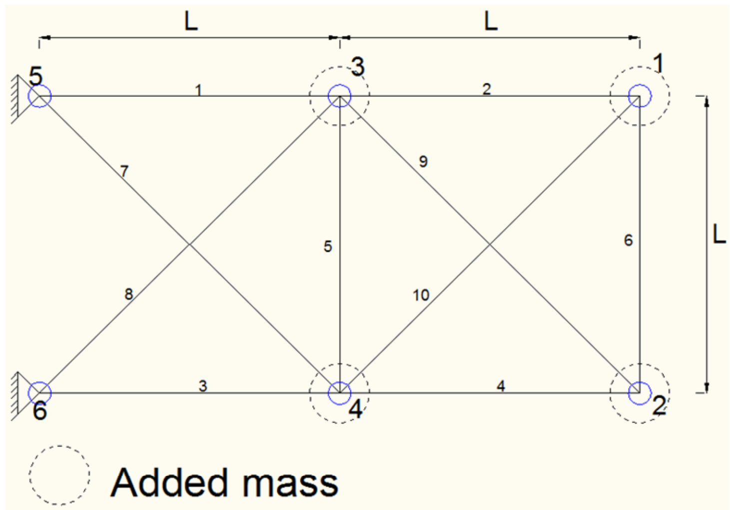


Figure 1. A ten-bar planar truss

Table 1: Material properties, variable bounds and frequency constraints for the 10-bar truss structure

| Property/unit | Value |
|---|---|
| E (Modulus of elasticity)/ N/m$^2$ | $6.98 \times 10^{10}$ |
| ρ (Material density)/ kg/m$^3$ | 2770.0 |
| Added mass/kg | 454.0 |
| Design variable lower bound/m$^2$ | $0.645 \times 10^{-4}$ |
| L (Main bar's dimension)/m | 9.144 |
| Constraints on first three frequencies/Hz | $\omega_1 \geq 7$, $\omega_2 \geq 15$, $\omega_3 \geq 20$ |

Table 2 represents the design vectors and the mass of the corresponding structures obtained by different researchers. It can be seen that both standard CSS and its enhanced version have outperformed their rivals.

Table 3 represents the natural frequencies of the optimized structures obtained by different researchers. It can be seen that all of the constraints are satisfied with an exception of the structure obtaized by Sedaghati et al. [10].

Table 2: Optimal design cross sections ($cm^2$) for several methods for the ten bar planar truss (weight does not include added masses)

| Element number | Grandhi & Venkayya [9] | Sedaghati et al. [10] | Wang et al. [11] | Lingyun et al. [12] | Gomes [13] | Present work | |
|---|---|---|---|---|---|---|---|
| | | | | | | Standard CSS | Enhanced CSS |
| 1 | 36.584 | 38.245 | 32.456 | 42.23 | 37.712 | 38.811 | 39.569 |
| 2 | 24.658 | 9.916 | 16.577 | 18.555 | 9.959 | 9.0307 | 16.740 |
| 3 | 36.584 | 38.619 | 32.456 | 38.851 | 40.265 | 37.099 | 34.361 |
| 4 | 24.658 | 18.232 | 16.577 | 11.222 | 16.788 | 18.479 | 12.994 |
| 5 | 4.167 | 4.419 | 2.115 | 4.783 | 11.576 | 4.479 | 0.645 |
| 6 | 2.070 | 4.419 | 4.467 | 4.451 | 3.955 | 4.205 | 4.802 |
| 7 | 27.032 | 20.097 | 22.810 | 21.049 | 25.308 | 20.842 | 26.182 |
| 8 | 27.032 | 24.097 | 22.810 | 20.949 | 21.613 | 23.023 | 21.260 |
| 9 | 10.346 | 13.890 | 17.490 | 10.257 | 11.576 | 13.763 | 11.766 |
| 10 | 10.346 | 11.452 | 17.490 | 14.342 | 11.186 | 11.414 | 11.392 |
| Weight(kg) | 594.0 | 537.01 | 553.8 | 542.75 | 537.98 | 531.95 | 529.25 |

Table 3: Natural frequencies (Hz) of the optimized structures (the ten-bar planar truss)

| Frequency number | Grandhi & Venkayya [9] | Sedaghati et al. [10] | Wang et al. [11] | Lingyun et al. [12] | Gomes [13] | Present work | |
|---|---|---|---|---|---|---|---|
| | | | | | | Standard CSS | Enhanced CSS |
| 1 | 7.059 | 6.992 | 7.011 | 7.008 | 7.000 | 7.000 | 7.000 |
| 2 | 15.895 | 17.599 | 17.302 | 18.148 | 17.786 | 17.442 | 16.238 |
| 3 | 20.425 | 19.973 | 20.001 | 20.000 | 20.000 | 20.031 | 20.000 |
| 4 | 21.528 | 19.977 | 20.100 | 20.508 | 20.063 | 20.208 | 20.361 |
| 5 | 28.978 | 28. 173 | 30.869 | 27.797 | 27.776 | 28.261 | 28.121 |
| 6 | 30.189 | 31.029 | 32.666 | 31.281 | 30.939 | 31.139 | 28.610 |
| 7 | 54.286 | 47.628 | 48.282 | 48.304 | 47.297 | 47.704 | 48.390 |
| 8 | 56.546 | 52.292 | 52.306 | 53.306 | 52.286 | 52.420 | 52.291 |

Table 4 summarizes the statistical results of ten independent runs together with the parameters used, for both original and enhanced CSS in order to optimize the ten bar planar truss.

Table 4: Statistical results of ten independent runs together with the parameters (the ten-bar truss)

| | **Mean weight (kg)** | **Standard deviation** | **Number of particles** | **$c_1$** | **$c_2$** |
|---|---|---|---|---|---|
| Standard CSS | 536.39 | 3.32 | 20 | 1 | 5 |
| Enhanced CSS | 538.53 | 5.97 | 20 | 1 | 5 |

Figure 2 shows the convergence curves for both original and enhanced CSS for the ten-bar planar truss.

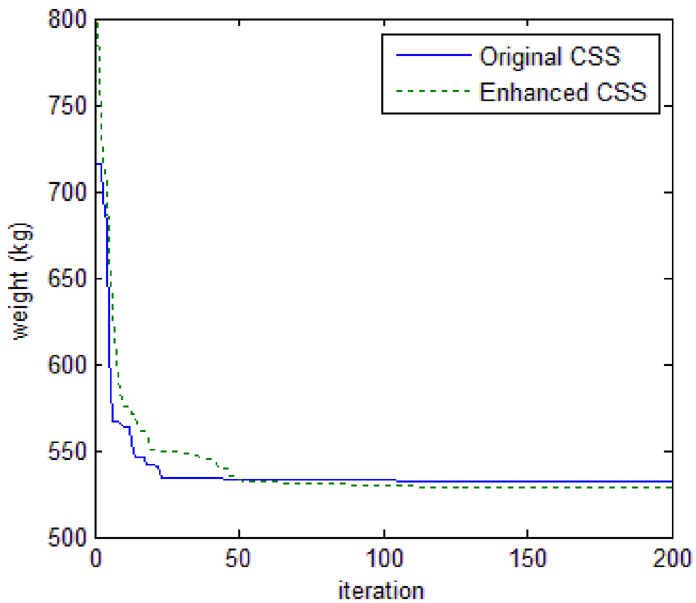


Figure 2. The convergence curves for the standard CSS and the enhanced CSS (the ten-bar planar truss)

*4.2 A 72-bar space truss*

Topology and element numbering of a 72-bar space truss is depicted in Figure 3. The elements are classified in 16 design groups according to Table 6. Four non-structural masses of 2270 kg are attached to the nodes 1 through 4. The predefined shape of the structure remains unchanged during the optimization process, so this is a sizing optimization problem with 16 variables. This example has been solved by Konzelman [14] using a dual method (DM) and by Sedaghati et al. [15] employing the force method (FM). Gomes [13] has investigated the problem using the particle swarm optimization.

Material properties, variable bounds, frequency constrains and added masses are listed in Table 5.

Table 5: Material properties and frequency constraints for the 72-bar space truss

| Property/unit | Value |
|---|---|
| E (Modulus of elasticity)/ $N/m^2$ | $6.98 \times 10^{10}$ |
| ρ (Material density)/ $kg/m^3$ | 2770.0 |
| Added mass/kg | 2270 |
| Design variable lower bound/$m^2$ | $0.645 \times 10^{-4}$ |
| Constraints on first three frequencies/Hz | $\omega_1$=4.0 , $\omega_3 \geq 6$ |

Table 6 shows the final cross-sectional areas for the 72-bar space truss obtained by different researchers together with the results gained by the CSS and its enhanced version.

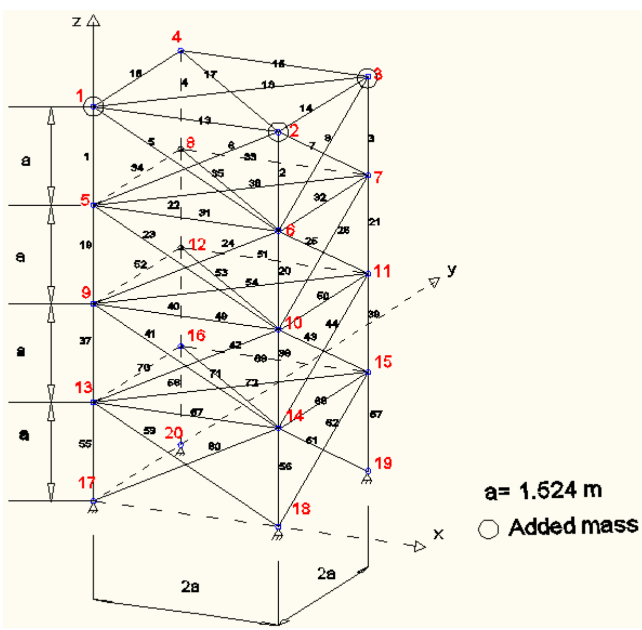


Figure 3. A 72-bar space truss

Table 6: Final cross-sectional areas for the 72-bar space truss ($cm^2$)

| Element group | Konzelman [14] | Sedaghati [15] | Gomes [13] | Present work | |
|---|---|---|---|---|---|
| | | | | Standard CSS | Enhanced CSS |
| 1–4 | 3.499 | 3.499 | 2.987 | 2.528 | 2.252 |
| 5–12 | 7.932 | 7.932 | 7.849 | 8.704 | 9.109 |
| 13–16 | 0.645 | 0.645 | 0.645 | 0.645 | 0.648 |
| 17–18 | 0.645 | 0.645 | 0.645 | 0.645 | 0.645 |
| 19–22 | 8.056 | 8.056 | 8.765 | 8.283 | 7.946 |
| 23–30 | 8.011 | 8.011 | 8.153 | 7.888 | 7.703 |
| 31–34 | 0.645 | 0.645 | 0.645 | 0.645 | 0.647 |
| 35–36 | 0.645 | 0.645 | 0.645 | 0.645 | 0.646 |
| 37–40 | 12.812 | 12.812 | 13.450 | 14.666 | 13.465 |
| 41–48 | 8.061 | 8.061 | 8.073 | 6.793 | 8.250 |
| 49–52 | 0.645 | 0.645 | 0.645 | 0.645 | 0.645 |
| 53-54 | 0.645 | 0.645 | 0.645 | 0.645 | 0.646 |
| 55–58 | 17.279 | 17.279 | 16.684 | 16.464 | 18.368 |
| 59–66 | 8.088 | 8.088 | 8.159 | 8.809 | 7.053 |
| 67-70 | 0.645 | 0.645 | 0.645 | 0.645 | 0.645 |
| 71-72 | 0.645 | 0.645 | 0.645 | 0.645 | 0.646 |
| Weight (kg) | 327.605 | 327.605 | 328.823 | 328.814 | 328.393 |

The structures resulted here are slightly lighter than that of Gomes [13] and slightly heavier than the solutions gained by Konzelman [14] and Sedaghati [15]. However, they seem to satisfy the first constraint better than their rivals; The first natural frequency is supposed to be equal to 4 while our analysis program evaluates it as 4.021, 4021 and 4.026 for the structures obtained by Konzelman[14], Sedaghati [15] and Gomes [13], respectively.

Table 7 represents the natural frequencies obtained by various methods for the 72-bar space truss. None of the constraints are violated according to Table 7.

Table 7: Natural frequencies (Hz) obtained by various methods for the 72-bar space truss

| Element group | Konzelman [14] | Sedaghati [15] | Gomes [13] | Present work | |
|---|---|---|---|---|---|
| | | | | Standard CSS | Enhanced CSS |
| 1 | 4.000 | 4.000 | 4.000 | 4.000 | 4.000 |
| 2 | 4.000 | 4.000 | 4.000 | 4.000 | 4.000 |
| 3 | 6.000 | 6.000 | 6.000 | 6.006 | 6.004 |
| 4 | 6.247 | 6.247 | 6.219 | 6.210 | 6.155 |
| 5 | 9.074 | 9.074 | 8.976 | 8.684 | 8.390 |

Figure 4 shows the convergence curves for both original and enhanced CSS for the 72-bar space truss.

Table 8 represents the statistical results of ten independent runs together with the parameters used, for both original and enhanced CSS in order to optimize the 72-bar space truss.

Table 8: Statistical results of ten independent runs together with the parameters (the 72-bar space truss)

| | **Mean weight (kg)** | **Standard deviation** | **Number of particles** | $c_1$ | $c_2$ |
|---|---|---|---|---|---|
| Standard CSS | 337.70 | 5.42 | 20 | 1 | 16 |
| Enhanced CSS | 335.77 | 7.20 | 20 | 1 | 16 |

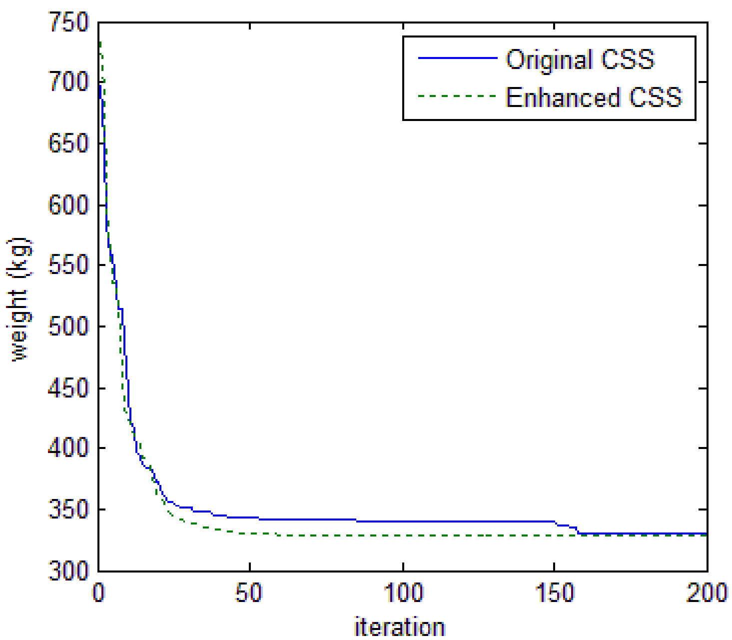


Figure 4. The convergence curves for both original and enhanced CSS (the 72-bar space truss)

### *4.3 A Simply supported 37-bar planar truss*

A simply supported 37-bar Pratt type truss, as depicted in Figure 5, is considered as the third example. The elements of the lower chord are modeled as bar elements with constant rectangular cross-sectional areas of $4\times10^{-3}$ m$^2$. The other bars are modeled as bar elements with initial cross-sectional areas of $1\times10^{-4}$ m$^2$. These members are grouped in a symmetrical manner to form the sizing variables. The y-coordinate of all the nodes on the upper chord can vary with respect to symmetry. A non-structural mass of 10 kg is attached at each of the free nodes of the lower chord. The first three natural frequencies of the structure are considered as the constraints. Thus this is an optimization on shape and size with nineteen design variables (fourteen sizing variables plus five shape variables) and three frequency constraints. This example has been investigated by Wang et al. [11] using an evolutionary node shift method and Lingyun et al. [12] employing a niche hybrid genetic algorithm. Gomes has analyzed this problem using the particle swarm algorithm [13].

Material properties, frequency constrains and added masses are listed in Table 9.

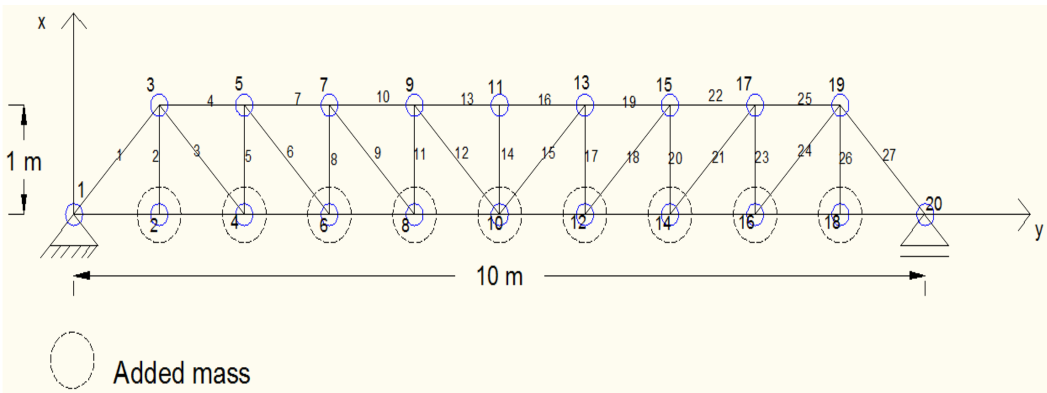


Figure 5. A simply supported 37-bar planar truss

Table 9: Material properties and frequency constraints for the 37-bar simply supported planar truss

| Property/unit | Value |
|---|---|
| E (Modulus of elasticity)/ $N/m^2$ | $2.1\times 10^{11}$ |
| ρ (Material density)/ $kg/m^3$ | 7800 |
| Added mass/kg | 10 |
| Constraints on first three frequencies/Hz | $\omega_1 \geq 20$, $\omega_2 \geq 40$, $\omega_3 \geq 60$ |

Table 10 represents a comparison between the cross-sectional areas and node coordinates obtained by different researchers together with the corresponding weight. It can be seen that both standard CSS and its enhanced form performed better than other optimization techniques and found lighter structures while satisfying all the constraints.

Table 10: Final cross-sectional areas and node coordinates for the 37-bar simply supported planar truss

| Variable | initial | Wang et al. [11] | Lingyun et al. [12] | Gomes [13] | Present work | |
|---|---|---|---|---|---|---|
| | | | | | Standard CSS | Enhanced CSS |
| Y3 , Y19 (m) | 1.0 | 1.2086 | 1.1998 | 0.9637 | 0.8726 | 1.0289 |
| Y5 , Y17 (m) | 1.0 | 1.5788 | 1.6553 | 1.3978 | 1.2129 | 1.3868 |
| Y7 , Y15 (m) | 1.0 | 1.6719 | 1.9652 | 1.5929 | 1.3826 | 1.5893 |
| Y9 , Y13 (m) | 1.0 | 1.7703 | 2.0737 | 1.8812 | 1.4706 | 1.6405 |
| Y11 (m) | 1.0 | 1.8502 | 2.3050 | 2.0856 | 1.5683 | 1.6835 |
| A1, A27 ($cm^2$) | 1.0 | 3.2508 | 2.8932 | 2.6797 | 2.9082 | 3.4484 |
| A2, A26 ($cm^2$) | 1.0 | 1.2364 | 1.1201 | 1.1568 | 1.0212 | 1.5045 |
| A3, A24 ($cm^2$) | 1.0 | 1.0000 | 1.0000 | 2.3476 | 1.0363 | 1.0039 |
| A4, A25 ($cm^2$) | 1.0 | 2.5386 | 1.8655 | 1.7182 | 3.9147 | 2.5533 |
| A5, A23 ($cm^2$) | 1.0 | 1.3714 | 1.5962 | 1.2751 | 1.0025 | 1.0868 |
| A6, A21 ($cm^2$) | 1.0 | 1.3681 | 1.2642 | 1.4819 | 1.2167 | 1.3382 |
| A7, A22 ($cm^2$) | 1.0 | 2.4290 | 1.8254 | 4.6850 | 2.7146 | 3.1626 |
| A8, A20 ($cm^2$) | 1.0 | 1.6522 | 2.0009 | 1.1246 | 1.2663 | 2.2664 |
| A9, A18 ($cm^2$) | 1.0 | 1.8257 | 1.9526 | 2.1214 | 1.8006 | 1.2668 |
| A10, A19 ($cm^2$) | 1.0 | 2.3022 | 1.9705 | 3.8600 | 4.0274 | 1.7518 |
| A11, A17 ($cm^2$) | 1.0 | 1.3103 | 1.8294 | 2.9817 | 1.3364 | 2.7789 |
| A12, A15 ($cm^2$) | 1.0 | 1.4067 | 1.2358 | 1.2021 | 1.0548 | 1.4209 |
| A13, A16 ($cm^2$) | 1.0 | 2.1896 | 1.4049 | 1.2563 | 2.8116 | 1.0100 |
| A14 ($cm^2$) | 1.0 | 1.0000 | 1.0000 | 3.3276 | 1.1702 | 2.2919 |
| Weight (kg) | 336.3 | 366.50 | 368.84 | 377.20 | 362.84 | 362.38 |

Table 11 shows the natural frequencies obtained by various methods for the 37-bar simply supported planar truss. None of the constraints are violated according to Table 11.

Table 11: Natural frequencies (Hz) obtained by various methods for the 37-bar simply supported planar truss

| Frequency number | initial | Wang et al. [11] | Lingyun et al. [12] | Gomes [13] | Present work | |
|---|---|---|---|---|---|---|
| | | | | | Standard CSS | Enhance d CSS |
| 1 | 8.89 | 20.0850 | 20.0013 | 20.0001 | 20.0000 | 20.0028 |
| 2 | 28.82 | 42.0743 | 40.0305 | 40.0003 | 40.0693 | 40.0155 |
| 3 | 46.92 | 62.9383 | 60.0000 | 60.0001 | 60.6982 | 61.2798 |
| 4 | 63.62 | 74.4539 | 73.0444 | 73.0440 | 75.7339 | 78.1100 |
| 5 | 76.87 | 90.0576 | 89.8244 | 89.8240 | 97.6137 | 98.4100 |

Table 12 summarizes the statistical results of ten independent runs together with the parameters used, for both original and enhanced CSS in order to optimize the 37-bar simply supported planar truss.

Table 12: Statistical results of ten independent runs together with the parameters (the 37-bar truss)

| | **Mean weight (kg)** | **Standard deviation** | **Number of particles** | $c_1$ | $c_2$ |
|---|---|---|---|---|---|
| Standard CSS | 366.77 | 3.742 | 20 | 1 | 7 |
| Enhanced CSS | 365.75 | 3.461 | 20 | 1 | 7 |

Figures 6 through 10 represent final shapes of the optimized structures obtained by different methods.

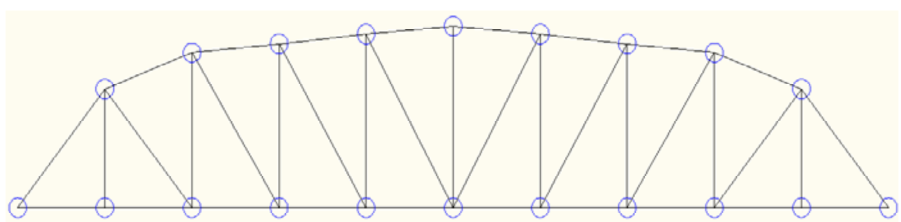

Figure 6. A 37-bar structure optimized by Wang [11].

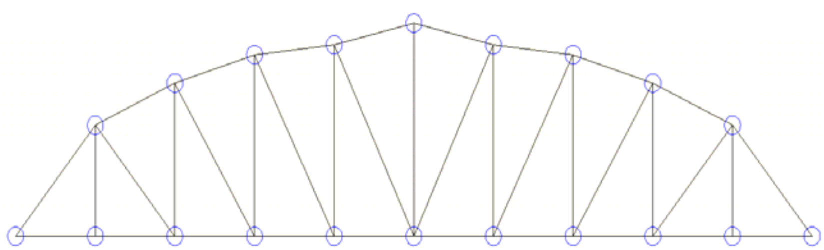

Figure 7. The 37-bar structure optimized by Lingyun et al. [12].

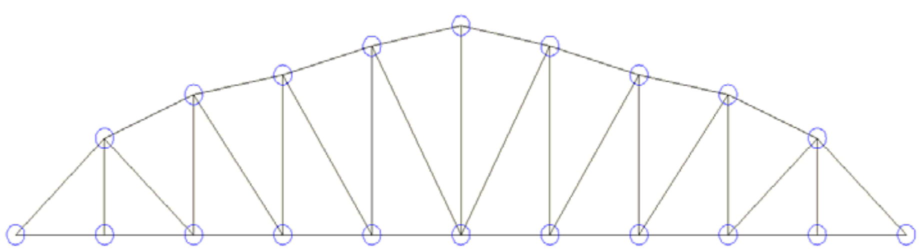

Figure 8. The 37-bar structure optimized by Gomes [13]

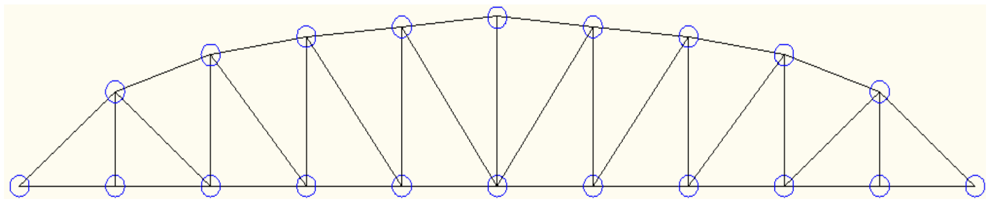

Figure 9. The 37-bar structure optimized by CSS

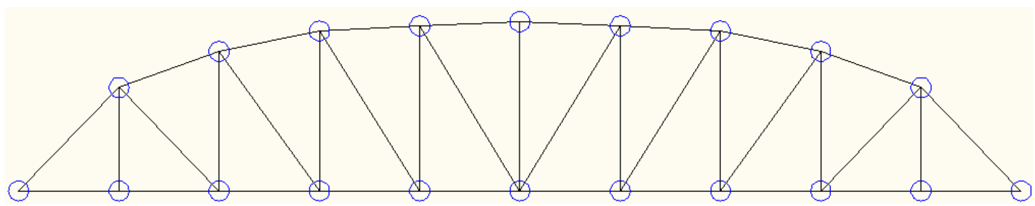

Figure 10. The 37-bar structure optimized by enhanced CSS

Figure 11 shows the convergence curves for both the original and the enhanced CSS for the 37-bar simply supported truss.

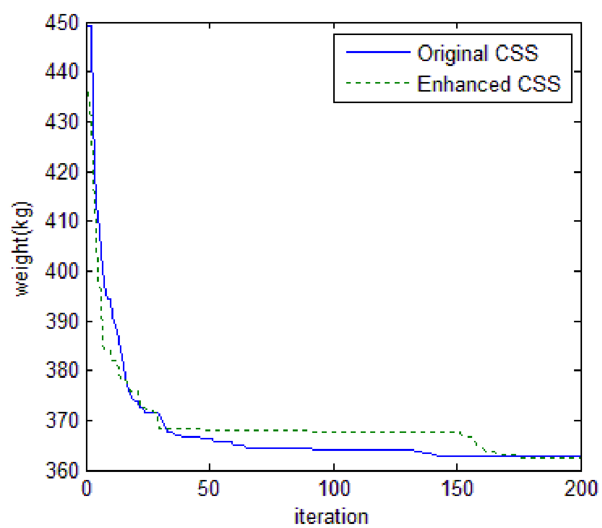


Figure 11. The convergence curves for both standard and enhanced CSS (the 37-bar simply supported truss)

*4.4 A 52-bar space truss*

A 52-bar dome-like space truss, as depicted in Figure 12, is considered as the last example. Non-structural masses of 50 kg are attached to all free nodes. Material properties, frequency constraints and variable bounds for this example are summarized in Table 13. All of the elements of the structure are categorized in 8 groups according to Table 14.

All free nodes are permitted to move in a symmetrical manner, they can move ±2m in each allowable direction from their initial position. Constraints are imposed on the first two natural frequencies.

So this is an optimization on shape and size with thirteen variables (eight sizing variables + five shape variables) and two frequency constraints. This example has been investigated by Lin et al. using a mathematical programming technique [16] and Lingyun et al. using a niche hybrid genetic algorithm [12]. Gomes has analyzed this problem using the particle swarm algorithm [13].

Table 13: Material properties and frequency constraints and variable bounds for the 52-bar space truss

| **Property/unit** | **Value** |
|---|---|
| E (Modulus of elasticity)/ N/m$^2$ | $2.1\times 10^{11}$ |
| ρ (Material density)/ kg/m$^3$ | 7800 |
| Added mass/kg | 50 |
| Allowable range for cross-sections/ m$^2$ | $0.0001\leq A\leq 0.001$ |
| Constraints on first three frequencies/Hz | $\omega_1\leq 15.916$ $\omega_2\geq 28.648$ |

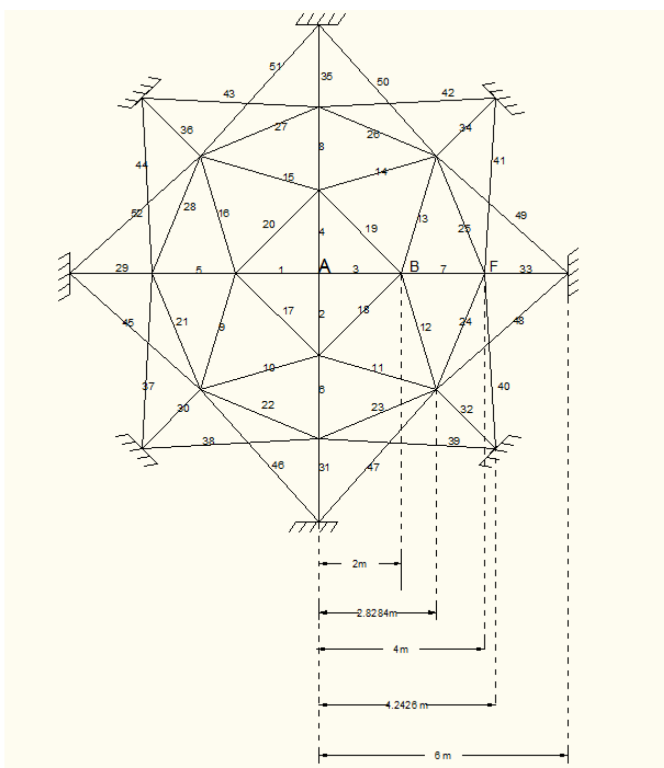


Figure 12. A 52-bar dome-like space truss (initial shape) a) top view

Table 14: Element grouping

| Group number | Elements |
|---|---|
| 1 | 1-4 |
| 2 | 5-8 |
| 3 | 9-16 |
| 4 | 17-20 |
| 5 | 21-28 |
| 6 | 29-36 |
| 7 | 37-44 |
| 8 | 45-52 |

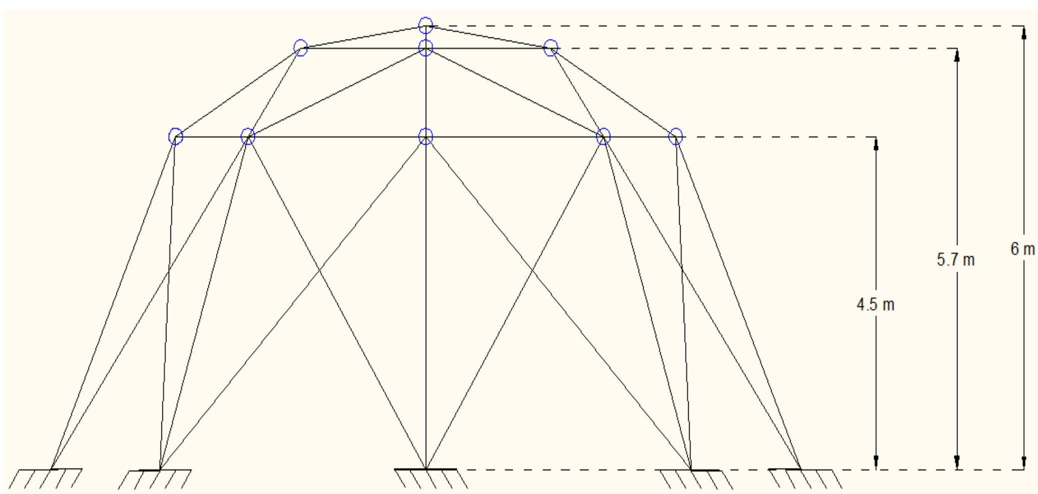


Figure 12. a) A 52-bar dome-like space truss (initial shape) b) side view

Table 15 represents a comparison between the cross-sectional areas and node coordinates obtained by different researchers together with the corresponding weight for the 52 bar space truss.

Table 15: Cross-sectional areas and node coordinates obtained by different researchers (the 52-bar space truss)

| **Variable** | **Initial** | **Liuet al. [16]** | **Lingyun et al. [12]** | **Gomes [13]** | **Present work** | |
|---|---|---|---|---|---|---|
| | | | | | **Standard CSS** | **Enhanced CSS** |
| $Z_A$ (m) | 6.000 | 4.3201 | 5.8851 | 5.5344 | 5.2716 | 6.1590 |
| $X_B$ (m) | 2.000 | 1.3153 | 1.7623 | 2.0885 | 1.5909 | 2.2609 |
| $Z_B$ (m) | 5.700 | 4.1740 | 4.4091 | 3.9283 | 3.7093 | 3.9154 |
| $X_F$ (m) | 4.000 | 2.9169 | 3.4406 | 4.0255 | 3.5595 | 4.0836 |
| $Z_F$ (m) | 4.500 | 3.2676 | 3.1874 | 2.4575 | 2.5757 | 2.5106 |
| A1 ($cm^2$) | 2.0 | 1.00 | 1.0000 | 0.3696 | 1.0464 | 1.0335 |
| A2 ($cm^2$) | 2.0 | 1.33 | 2.1417 | 4.1912 | 1.7295 | 1.0960 |
| A3 ($cm^2$) | 2.0 | 1.58 | 1.4858 | 1.5123 | 1.6507 | 1.2449 |
| A4 ($cm^2$) | 2.0 | 1.00 | 1.4018 | 1.5620 | 1.5059 | 1.2358 |
| A5 ($cm^2$) | 2.0 | 1.71 | 1.911 | 1.9154 | 1.7210 | 1.4078 |
| A6 ($cm^2$) | 2.0 | 1.54 | 1.0109 | 1.1315 | 1.0020 | 1.0022 |
| A7 ($cm^2$) | 2.0 | 2.65 | 1.4693 | 1.8233 | 1.7415 | 1.6024 |
| A8 ($cm^2$) | 2.0 | 2.87 | 2.1411 | 1.0904 | 1.2555 | 1.4596 |
| Weight (kg) | 338.69 | 298.0 | 236.046 | 228.381 | 205.237 | 197.337 |

Table 16 shows the natural frequencies obtained by various methods for the 52-bar dome-like space truss.

Table 16: Natural frequencies (Hz) obtained by various methods (the 52-bar space truss)

| **Frequency number** | **Initial** | **Liu et al. [16]** | **Lingyun et al. [12]** | **Gomes [13]** | **Present work** | |
|---|---|---|---|---|---|---|
| | | | | | **Standard CSS** | **Enhanced CSS** |
| 1 | 22.69 | 15.22 | 12.81 | 12.751 | 9.246 | 11.849 |
| 2 | 25.17 | 29.28 | 28.65 | 28.649 | 28.648 | 28.649 |
| 3 | 25.17 | 29.28 | 28.65 | 28.649 | 28.699 | 28.659 |
| 4 | 31.52 | 31.68 | 29.54 | 28.803 | 28.735 | 28.718 |
| 5 | 33.80 | 33.15 | 30.24 | 29.230 | 29.223 | 29.192 |

Table 17 represents the statistical results of ten independent runs together with the parameters used, for both original and enhanced CSS in order to optimize the 52-bar dome-like space truss.

Table 17: Statistical results of ten independent runs together with the parameters (the 52-bar truss)

| | **Mean weight (kg)** | **Standard deviation** | **Number of particles** | $c_1$ | $c_2$ |
|---|---|---|---|---|---|
| Standard CSS | 213.101 | 7.391 | 20 | 1 | 7 |
| Enhanced CSS | 205.617 | 6.924 | 20 | 1 | 7 |

Figure 13 shows the convergence curves for both original and enhanced CSS for the 52-bar space truss.

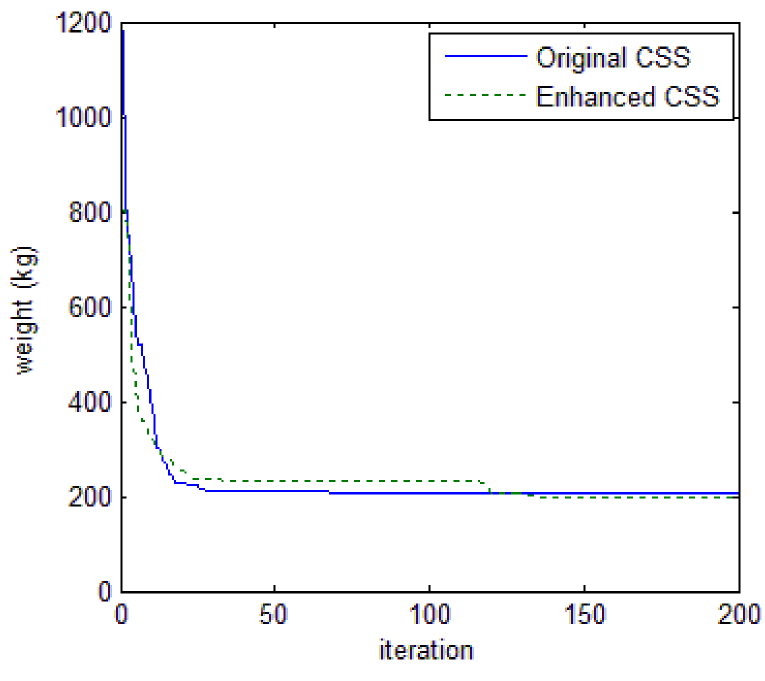


Figure 13. The convergence curves for both original and enhanced CSS for the 52-bar space truss

Figures 14 and 15 represent the optimized shape of the 52-bar dome-like truss obtained by the standard CSS and its enhanced form.

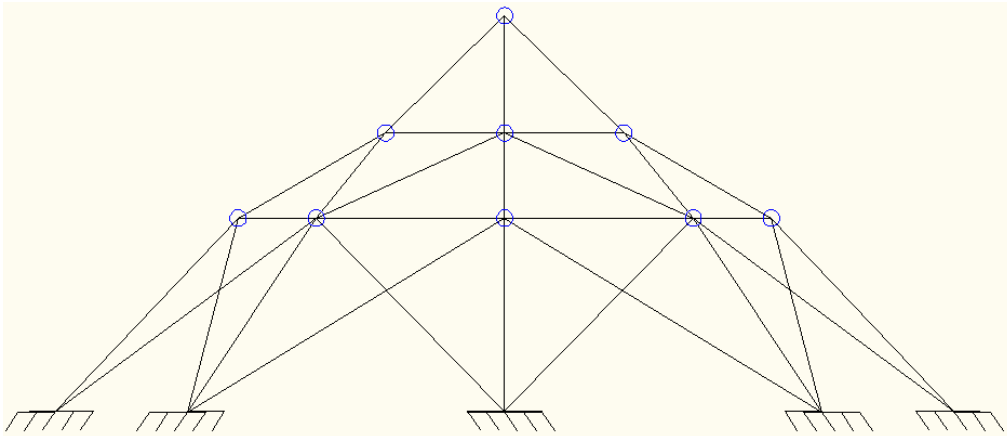

Figures 14. The optimized shape of the 52-bar dome-like space truss (the standard CSS)

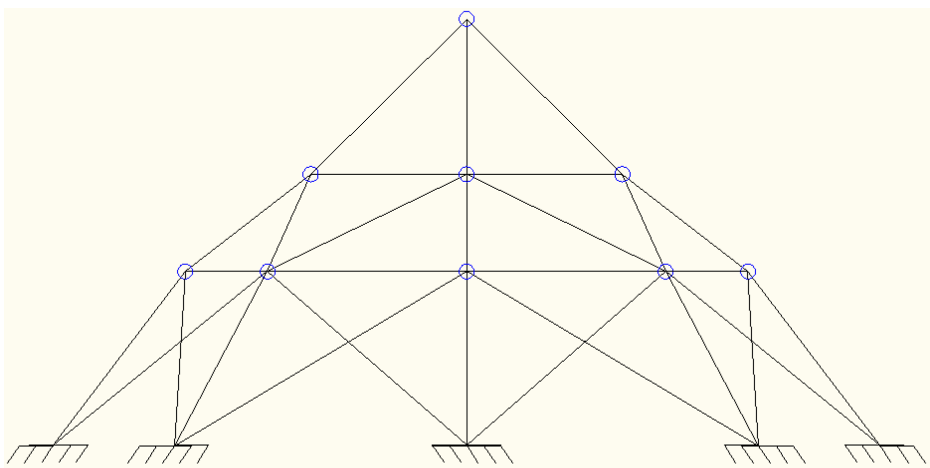

Figures 15. The optimized shape of the 52-bar dome-like space truss (the enhanced CSS)

## 5. CONCLUDING REMARKS

In this paper frequency constraint optimization of truss structures on shape and size is studied. This kind of problem has a highly non-linear behavior because of the different nature of the variables involved, their different order and the sensitivity of the natural frequencies to shape modifications. Here, the newly developed the CSS algorithm and its enhanced form are utilized to find the optimum design of the structures. The frequency constraints are handled using the well-known penalty approach.

CSS is a multi-agent metaheuristic algorithm which utilizes the Coulomb and Gauss laws of electrostatics and some laws of Newtonian mechanics to improve the solutions iteratively. Apart from the well-known advantages of metaheuristic algorithms compared to classical optimization techniques, CSS has an important feature which increases the probability of finding better results; it can distinguish finishing the global phase and change the movement updating equation for the local phase to have a better balance between the exploration and exploitation [4].

Form the results of this study it can be seen that both standard CSS and its enhanced form have performed better than the other methods available in the literature in three of the four examples considered, and in the other example the structure is only slightly heavier than the best one found.

**Acknowledgment:** The first author is grateful to the Iranian Academy of Sciences for the support.

## REFERENCES

1. Gholizadeh S, Salajegheh E, and Torkazadeh P. Structural optimization with frequency constraints by genetic algorithm using wavelet radial basis function neural network, *Journal of Sound and Vibration* **312**(2008)316–31.
2. Grandhi RV. Structural optimization with frequency constraints – A review. *AIAA Journal* **31**(12) (1993)2296–303.
3. Kaveh A, and Talatahari S. A novel heuristic optimization method: charged system search, *Acta Mechanica* **213**(3-4) (2010) 267-89.
4. Kaveh A, and Talatahari S. Optimal design of skeletal structures via the charged system search algorithm, *Structural and Multidisciplinary Optimization* **41**(6) (2010)893-911.
5. Kaveh A, and Talatahari S. An enhanced charged system search for configuration optimization using the concept of field of forces, *Structural and Multidisciplinary Optimization* DOI 10.1007/s00158-010-0571-1.
6. Halliday D, Resnick R, and Walker J. *Fundamentals of Physics*, 8th ed, John Wiley and Sons; 2008.
7. Kaveh A, and Talatahari S. Charged system search for optimum grillage system design using the LRFD-AISC code, *Journal of Constructional Steel Research* **66**(2010)767-71.
8. Kaveh A, and Talatahari S. Particle swarm optimizer, ant colony strategy and harmony search scheme hybridized for optimization of truss structures, *Computers and Structures* **87**(56) (2009)267-83.
9. Grandhi RV, and Venkayya VB. Structural optimization with frequency constraints. *AIAA Journal* **26**(7) (1988)858–66.
10. Sedaghati R, Suleman A, and Tabarrok B. Structural optimization with frequency constraints using finite element force method, *AIAA Journal* **40**(2) (2002)382–8.
11. Wang D, Zhang WH, and Jiang JS. Truss optimization on shape and sizing with frequency constraints. *AIAA Journal* **42**(3) (2004)1452–6.
12. Lingyun W, Mei Z, Guangming W, and Guang M. Truss optimization on shape and sizing with frequency constraints based on genetic algorithm, *Journal of Computational Mechanics* **25** (2005)361–8.
13. Gomes MH. Truss optimization with dynamic constraints using a particle swarm

algorithm, *Expert Systems with Applications* **38** (2011)957–68.
14. Konzelman CJ. Dual methods and approximation concepts for structural optimization. M.Sc. thesis, Department of Mechanical Engineering, University of Toronto (1986).
15. Sedaghati R. Benchmark case studies in structural design optimization using the force method. *International Journal of Solids and Structures* **42** (2005)5848–71.
16. Lin JH, Chen WY, and Yu YS. Structural optimization on geometrical configuration and element sizing with static and dynamic constraints. *Computers and Structures* **15**(5) (1982)507–15.